

## EPR GEOMETRIC FACTOR for CYLINDRICAL CELLS (TRG, revised 2/12/13)

The EPR shift arises from the shift in the Rb electron paramagnetic resonance frequency due to the magnetic field produced by the  $^3\text{He}$  in the cell[1]. For spherical cells, the magnetic field is constant and given by  $8\pi M_{\text{He}}/3$ , where  $M_{\text{He}}$  is the  $^3\text{He}$  magnetization. For non-spherical cells the ratio  $C(\vec{x}) = B_{\text{He}}/M_{\text{He}}$  varies with location, hence to determine the shift requires averaging  $C(\vec{x})$  over the atoms responding the EPR RF field and sampled by the laser light reaching the photodiode, which I will call  $\langle C \rangle$ . Since we are using the optical pumping light for EPR,  $\langle C \rangle$  depends on whether we are end pumping or side pumping cylindrical cells. For end-pumping, ie. laser light traveling along the cylindrical axis, an analytical form[2, 3] can be employed:

$$\langle C_{\text{end}} \rangle = \frac{8\pi}{3} \left( \frac{3}{2} \right) \left[ \sqrt{1 + \left( \frac{a}{l} \right)^2} - \frac{a}{l} \right] \quad (1)$$

where  $a$  is the radius of the cell. Fig. 1 shows  $\langle C \rangle$  vs.  $D/L$  for cylindrical cells, where  $D = 2a$  and  $L$  are the cylindrical cell's diameter and length, respectively. The blue curve is from Eq. (1). Note that application of this formula assumes that we are only sampling light traveling in a narrow beam along the  $z$ -axis of the cell and that all atoms along this line contribute equally to the dip in the the photodiode signal. We are also approximating the blown cell by a right circular cylinder. The solid blue squares show results from COMSOL[5], which agree reasonably well. (I used a 40 cm radius spherical volume and the preset "finer" resolution for the COMSOL modelling.) The points correspond to the dimensions for some of our cells, plus sample  $D/L$  ratios to populate the plot over a wide range. The spherical value  $C = 8\pi/3 = 8.378$  is shown as a red diamond.  $\langle C_{\text{end}} \rangle$  decreases from a maximum value of  $4\pi = 12.57$  for  $D/L = 0$  (infinitely long cylinder) down to zero for  $D/L = \infty$  (infinitely thin pancake cylinder); the spherical value is obtained for a cylinder with a diameter a bit smaller than its length ( $D/L \approx 0.83$ ).

For side pumping one needs to average over a laser beam path that crosses the center of the cell. We don't know of an analytical formula, although perhaps this could be worked out. (I looked at Bien Chann's thesis and it might be possible but would requires more complex Bessel function integrals than that required for end pumping.) The solid green circles show the side pumping results from COMSOL. The dotted green curve is a fit to a function I made up by tweeking the end-pumping formula a bit:

$$\langle C_{\text{side}}^{\text{fit}} \rangle = 4\pi + m_1 - \frac{8\pi}{3} \left( \frac{3}{4} \right) \left[ \sqrt{1 + \left( \frac{m_3 a}{l} \right)^2} - \frac{m_3 a}{l} \right] \quad (2)$$

where  $m_1 = -0.17574$  and  $m_3 = 0.59193$  were obtained by fitting to the COMSOL values in the plot.  $\langle C_{\text{end}} \rangle$  increases from a minimum value of  $2\pi = 6.28$  for  $D/L = 0$  (infinitely long cylinder) up to what I expect might approach  $4\pi = 12.57$  for  $D/L = \infty$  (infinitely thin pancake cylinder); the spherical value is obtained for a cylinder with a diameter  $\approx 1.57$  times its length ( $D/L \approx 1.57$ ). Based on this behavior, I made up Eq. (2) by subtracting half the end-pumping formula from  $4\pi$ , and then adding in a stretching parameter  $m_3$  for the shape, and a deviation  $m_1$  from  $4\pi$  at  $D/L = \infty$ .

The geometrical effect on the  $^3\text{He}$  polarization is relatively small. Fig. 2 shows  $\langle C \rangle$  for the restricted range  $0.4 < D/L < 2$  for typical cells. Alan used COMSOL to determine  $\langle C \rangle = 6.7$  for the wide-angle cells, as we typically pump them[4]. Fig. 3 shows the approximate fractional change in  $^3\text{He}$  polarization for  $\langle C \rangle$  between 6 and 12 (assuming a given measured frequency shift and  $\kappa_0 \approx 6.1$ ). The fractional change plotted is given by  $\kappa'/\kappa_0 = (\frac{3}{8\pi} \langle C \rangle - 1)/6.1$ . For an increase in  $\langle C \rangle$  of unity, one obtains  $\approx -2.0$  % change in  $^3\text{He}$  polarization.

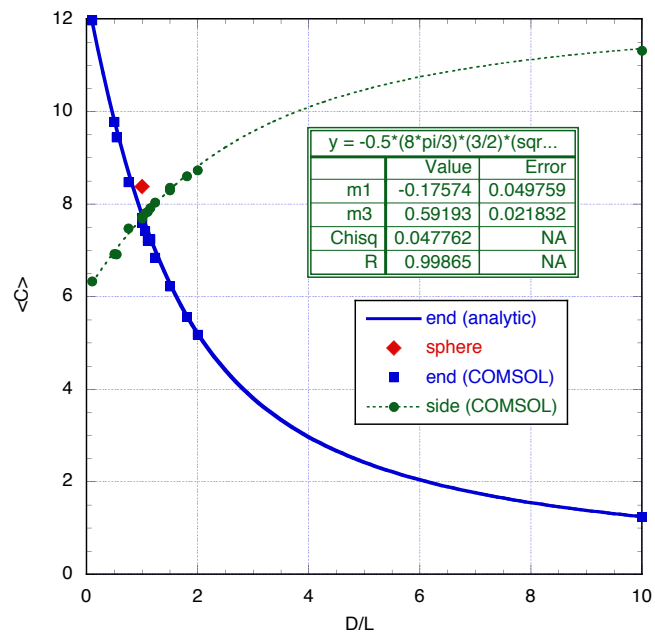


**Figure 1.** Variation of  $\langle C \rangle$  with  $D/L$ , where  $D$  and  $L$  are the cell's diameter length, respectively.

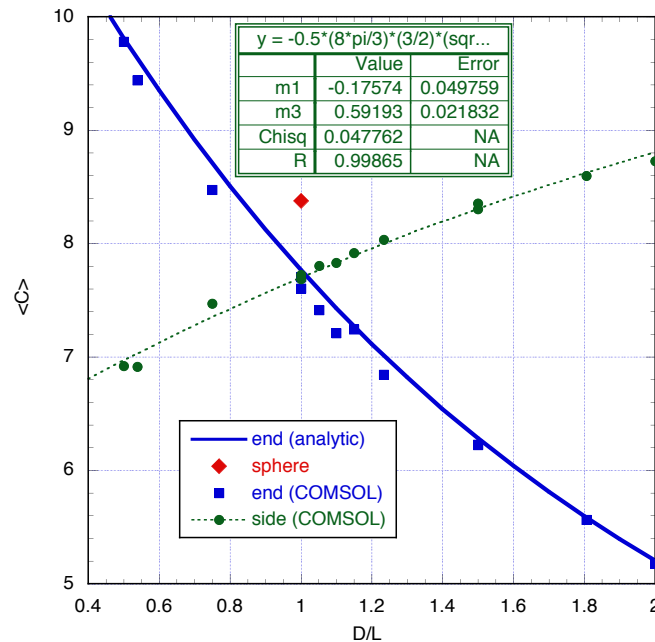


**Figure 2.** Variation of  $\langle C \rangle$  with  $D/L$  for the restricted range of typical cells

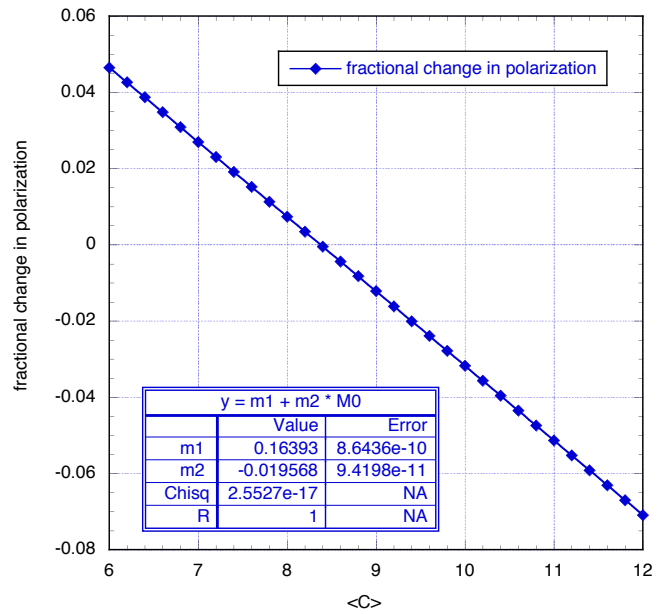


**Figure 3.** Fractional change in  $^3\text{He}$  polarization (assuming a given measured frequency shift and  $\kappa \approx 6.1$ ).

## References

- [1] M. V. Romalis and G. D. Cates, Phys. Rev. A **58**, 3004 (1998). “Accurate  $^3\text{He}$  polarimetry using the Rb Zeeman frequency shift due to the Rb- $^3\text{He}$  spin-exchange collisions”
- [2] B. Chann *et al.*, Phys. Rev. A **66**, 032703 (2002). “Measurements of  $^3\text{He}$  spin-exchange rates”
- [3] B. Chann. Ph.D. thesis, University of Wisconsin-Madison, 2003. “Studies of spin-exchange optical pumping”
- [4] Q. Ye *et al.*, Physics Procedia **42**, 206-212 (2013). “Wide angle polarization analysis with neutron spin filters”
- [5] COMSOL Multiphysics, COMSOL, Inc., Los Angeles, CA.